

FUS-MAE: A CROSS-ATTENTION-BASED DATA FUSION APPROACH FOR MASKED AUTOENCODERS IN REMOTE SENSING

Hugo Chan-To-Hing, Bharadwaj Veeravalli

National University of Singapore, Department of Electrical and Computer Engineering

ABSTRACT

This is a preprint for a submission to IGARSS 2024.

Self-supervised frameworks for representation learning have recently stirred up interest among the remote sensing community, given their potential to mitigate the high labeling costs associated with curating large satellite image datasets. In the realm of multimodal data fusion, while the often used contrastive learning methods can help bridging the domain gap between different sensor types, they rely on data augmentations techniques that require expertise and careful design, especially for multispectral remote sensing data. A possible but rather scarcely studied way to circumvent these limitations is to use a masked image modelling based pre-training strategy. In this paper, we introduce Fus-MAE, a self-supervised learning framework based on masked autoencoders that uses cross-attention to perform early and feature-level data fusion between synthetic aperture radar and multispectral optical data - two modalities with a significant domain gap. Our empirical findings demonstrate that Fus-MAE can effectively compete with contrastive learning strategies tailored for SAR-optical data fusion and outperforms other masked-autoencoders frameworks trained on a larger corpus.

Index Terms— Self-supervised learning, Masked Autoencoders, Cross-Attention, Data Fusion, SAR-optical

1. INTRODUCTION

Multi-modal learning has been attracting increasing attention over the past years, for a vast array of modalities such as RGB-Depth [1] or text-image [2]. Notably, recent research has established theoretical justifications for a performance edge of deep multi-modal learning over unimodal [3]. Within the domain data fusion for remote sensing (RS), two modalities are extensively studied: synthetic aperture radar (SAR) and optical imagery. Indeed, these modalities inherently complement each other: while SAR data offers all-weather and cloud-penetrating capabilities, it suffers from speckle noise, rendering its interpretation challenging. On the other hand, optical data, though subject to weather and seasonal constraints, proposes natural-looking (e.g. RGB) and less noisy images, facilitating interpretation. Hence, their combination

proves relevant for tasks such as land cover classification, and opens doors to applications like cloud removal [4] and SAR despeckling [5].

Self-supervised learning (SSL) has stirred substantial interest across diverse machine learning fields, such as natural language processing (NLP) [6, 7] and computer vision [8, 9]. One of its key characteristics is its ability to learn powerful representations without the need for labelled data, which is particularly interesting in the domain of RS, where data annotation can be costly and often requires specific expertise.

The increasing availability of large-scale public SAR-optical datasets such as SeCo [10], BigEarthNet-MM [11], SEN12MS [12] and, more recently, SSL4EO-12 [13] fostered research on SSL approaches for SAR-optical fusion. However, the majority of existing research leans towards contrastive learning [14], which, while effective, presents certain limitations. These include a reliance on data augmentations, which need to be carefully designed to adapt to the specificities of remote sensing images (RSI), as well as the necessity for negative samples, which necessitates a large batch size.

Recent advances in masked image modelling (MIM) [9] set a new state-of-the-art for some visual representation learning tasks. Despite MIM avoiding the aforementioned drawbacks of contrastive learning, to the best of our knowledge, the literature on data fusion for RSI using MIM remains relatively scarce [15, 16]. In this paper, we explore this alternative pretraining approach for SSL data fusion, with our contributions being summarized as following:

1. We introduce FusMAE, a self-supervised, MAE-based framework able to perform early-level as well as feature-level data fusion.
2. We demonstrate empirically that an early fusion strategy based on cross-attention is the most pre-training SAR-optical data fusion strategy for land cover classification tasks.
3. We show that our FusMAE model can compete with some of the most recent contrastive learning approaches tailored for RSI data fusion.

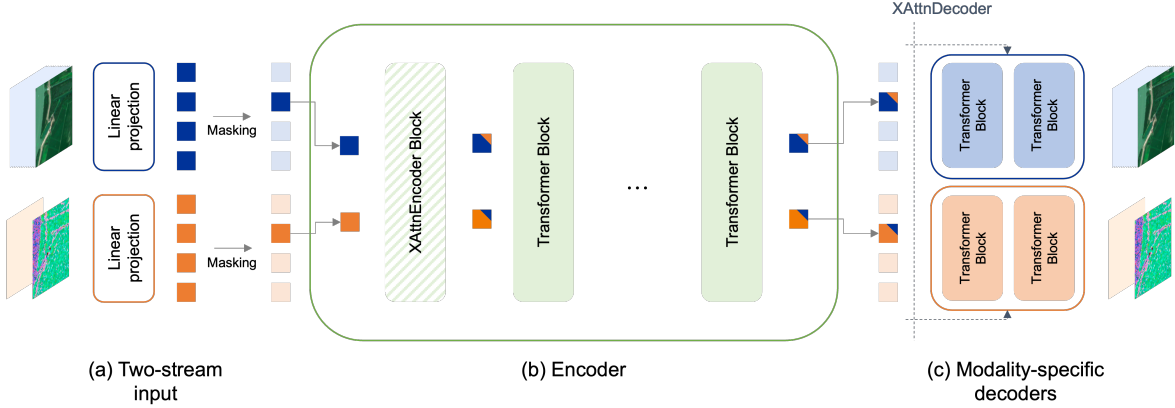


Fig. 1. Overall architecture of our Fus-MAE framework.

2. RELATED WORKS

Self-supervised learning in RS - As per in the literature [14], self-supervised learning methods can be classified into 3 categories: (1) generative methods, where the pretext task is to reconstruct a corrupted signal at pixel-level (e.g. downsampled [17] or masked [18]), (2) predictive methods, where the objective is to learn semantic context features through pretext tasks such as predicting the relative positions of two patches of an image (for spatial features) [19] or gray-to-RGB coloration (for spectral features) [20], and (3) contrastive learning methods, which traditionally aims at creating an embedding space where views of the same instance are drawn closer (positive views), while unrelated views are pulled apart (negative views) [21, 8]. For SAR-optical data fusion, most research efforts lean towards the latter: Chen and Bruzzone [22] studied early, intermediate and late fusion of SAR and optical images by jointly training two ResUnets with a multi-view contrastive loss. Montanaro et al. [23] used the SimCLR framework to bring the embeddings from different modalities closer. Wang et al. [24] adapted the knowledge distillation-based DINO framework [25], which doesn't require negative samples, getting rid of the need for a large batch size. While quite successful, all of these contrastive methods need a careful design of the data augmentation pipeline to create the positive views, whose quality can be difficult to assess. To bypass this challenge, we choose to focus on a generative method which doesn't require data augmentations: masked image modelling.

Masked image modelling in RS - He et al. [9] recently proposed a variation of the denoising autoencoder architecture (DAE), where input images patches are randomly masked with a high masking ratio, leaving only a small subset of patches to be fed into transformer encoder. Then, a shallow decoder reconstructs the image using both obtained latents and masked tokens. Called masked autoencoder (MAE), this framework set a new state-of-the-art on ImageNet-1K, while

accelerating training time considerably due to the lower number of processed input tokens and the lightweight decoder. Cong et al. [18] adapted this architecture for optical data by adding multi-domain encoding (e.g. positional+temporal or positional+spectral). Sun et al. [26] trained an MAE-based model on a 2M optical images dataset and claim to have achieved SOTA performance on various RS datasets. Allen et al. [27] followed up with a comparable work for SAR images. However, despite recent advancements on masked image modelling for data fusion on the natural domain [28], literature is less extensive for SAR-optical, with some attempts to train MAEs by stacking SAR and optical data along the channel axis [15] and some studies on specialized masking strategies [16]. In this paper, we propose some architectural changes to study early, intermediate and late fusion strategies to pave the way for further research.

3. METHODOLOGY

Our work is inspired from MultiMAE, a masked autoencoder-based architecture with a proven track record for natural images, able to take different modalities as input [28] with its hybrid-stream architecture. In this section, we describe the Fus-MAE architecture by motivating the need for a multi-task encoder in section 3.1 and a multi-task decoder in section 3.2. Two masking strategies are considered, with detailed provided in section 3.3. The overall architecture is shown in Figure 1.

3.1. Multi-modal encoder

As in MAE [9], our encoder is a ViT [29] and takes linearly embedded vector representations of patches as input tokens. Let $\mathbf{I}_1 \in \mathbb{R}^{H \times W \times C_1}$ and $\mathbf{I}_2 \in \mathbb{R}^{H \times W \times C_2}$ be the respective tensor representations of a SAR and an optical satellite image. An intuitive fusion strategy would be to stack SAR and optical RSI data along the channel dimension, and create patches

from the obtained tensor. Since this early concatenation technique focuses the entire fusion process onto the single patch projection layer, we hypothesize that it would not be expressive enough to effectively describe cross-modal interactions given the significant domain gap between SAR and optical data. To solve this challenging early fusion task, FusMAE replaces the first encoder block by a "Cross-attended patch projection" module, which encodes finer-grained multi-modal information into the input tokens. Code and model weights will be made publicly available on GitHub.

Cross-attended patch projection - We first create unimodal tokens using modality-specific patch projection layers. More specifically, given a patch size P , for each modality i , a 2D convolutional layer Conv2d_i of kernel size $P \times P$ and stride $P \times P$ is applied, and then positional embeddings \mathbf{E}_{emb} are added, to get a set of $(H/P)^2$ tokens $\mathbf{z}_{0,i}$:

$$\mathbf{z}_{0,i} = \text{Conv2d}_i(\mathbf{I}_i) + \mathbf{E}_{emb} \quad (1)$$

Then, to perform an early fusion operation, we introduce a block called XAttnEncoder (for cross-attention encoder), which is defined as:

$$\text{fus}(\mathbf{x}, \mathbf{y}) = \mathbf{x} \oplus \mathbf{y} + \text{CA}(\mathbf{x}, \mathbf{y}) \oplus \text{CA}(\mathbf{y}, \mathbf{x}) \quad (2)$$

$$\text{XAttnEncoder}(\mathbf{x}, \mathbf{y}) = \text{fus}(\mathbf{x}, \mathbf{y}) + \text{MLP}(\text{fus}(\mathbf{x}, \mathbf{y})) \quad (3)$$

with \oplus the concatenation operation, MLP a two layer feed-forward network with a GELU non-linearity, and CA a cross attention layer defined as:

$$\text{CA}(\mathbf{x}, \mathbf{y}) = \text{Attention}(\mathbf{Q}_x, \mathbf{K}_y, \mathbf{V}_y) \quad (4)$$

$$= \text{Softmax} \left(\frac{\mathbf{Q}_x \mathbf{K}_y^T}{\sqrt{d_q}} \right) \mathbf{V}_y \quad (5)$$

Our final set of input tokens \mathbf{z}_0 is obtained by feeding the sets of unimodal tokens to this XAttnEncoder block, as well as appending a global token z_{CLS} with learned embedding, similarly to [28]:

$$\mathbf{z}_0 = \text{XAttnEncoder}(\mathbf{z}_{0,1}, \mathbf{z}_{0,2}) \oplus z_{CLS} \quad (6)$$

The main idea behind the replacement of the first encoder block with this XAttnEncoder block is that, given the large domain gap between the two modalities, feeding both streams of unimodal tokens into the encoder block's self-attention layer would have resulted in an attention map akin to a block diagonal matrix, with poor cross-modality understanding. On the other hand, the XAttnEncoder block incites the network to model cross-modal interactions very early, creating tokens with unimodal bias as well as relevant cross-modal information [insert illustrations of attention map either here or in experiments section].

Modality-biased latents - Let N be the depth of our ViT encoder \mathcal{E}_N . In the case where the XAttnEncoder block is

used, \mathcal{E}_N encoder will be composed of one XAttnEncoder block followed by $N-1$ Transformer encoder blocks. We feed our unimodal tokens $\mathbf{z}_{0,i}$ to the encoder, to obtain a set of modality-biased latents \mathbf{z}_N , which can be decomposed as:

$$\mathbf{z}_n = \mathcal{E}_N(\mathbf{z}_{0,1}, \mathbf{z}_{0,2}) \quad (7)$$

$$= \mathbf{z}_{N,1} \oplus \mathbf{z}_{N,2} \quad (8)$$

3.2. Multi-task decoder

With the aim of performing feature-level data fusion, our architecture proposes to set up one encoder per modality. Following MAE [9], we use lightweight decoders, therefore adding decoders does not significantly increase the overall computational complexity of the model. We feed modality-biased latents $\mathbf{z}_{N,i}$ to their respective decoder \mathcal{D}_i , to obtain a reconstruction of the original RSI data $\hat{\mathbf{I}}_i$

$$\hat{\mathbf{I}}_i = \mathcal{D}_i(\mathbf{z}_{N,i}) \quad (9)$$

We then compute the Mean Square Error loss over the reconstructed tokens only, and backpropagate the gradients over the whole architecture.

To further insist on feature-level cross-modal information fusion, following MultiMAE [28], we introduce a XAttnDecoder block, which performs cross-attention between the modality-biased latents, before feeding them to \mathcal{D}_i :

$$\mathbf{z}^{\times}_{N,i} = \mathbf{z}_{N,i} + \text{CA}(\mathbf{z}_{N,i}, \mathbf{z}_{N,j}) \quad (10)$$

$$\text{XAttnDecoder}(\mathbf{z}_{N,i}) = \mathbf{z}^{\times}_{N,i} + \text{MLP}(\mathbf{z}^{\times}_{N,i}) \quad (11)$$

3.3. Masking strategies

We propose to study two masking strategies: independant masking and consistent masking. Following MAE [9], we apply a 75% masking ratio and sample our patches uniformly across modalities.

Independant masking - In the MiM for RS literature [18, 16], independent masking across modalities is widely adopted, as it enables to capture both inter- and intra- modalities correlations. Following this strategy, we randomly sample our masked patches uniformly across modalities.

Consistent masking - We also study a consistent masking strategy, where masked patches are the same across modalities. Our hypothesis is that, given the domain gap between SAR and optical data, capturing inter-modalities correlations is easier than intra-modalities. By guaranteeing that we feed tokens representing the same patches across modalities, we reduce the difficulty for the attention layers to capture cross-modal information.

	mAP - 100% labels			mAP - 1% labels		
	S1	S2	S1+S2	S1	S2	S1+S2
ImageNet	70,2	85,5	83,4	55,9	58,5	60,5
Dino-MM [24]	69,7	83,9	84,6	52,7	58,7	60,3
SatViT [15]	75,4	85,6	85,5	52,4	58,5	58,0
Fus-MAE w/ XAD	73,5	87,8	86,9	59,3	60,4	63,1
Fus-MAE w/ XAE&D	75,5	87,9	87,9	57,8	70,0	68,7

Table 1. Mean Average Precision results for the BigEarthNet-MM dataset. S1 = SAR data only. S2 = optical data only. S1+S2 = SAR-optical data fusion. XAD = XAttnDecoder, XAE&D = XAttnEncoder&Decoder.

	Top1-Acc	Top3-Acc	Precision	Recall	F1-score
ImageNet	58,6	90,7	75,2	58,6	60,1
Dino-MM [24]	58,8	91,0	71,4	58,8	59,7
SatViT [15]	59,1	91,8	75,2	59,1	59,9
Fus-MAE w/ XAD	59,8	92,4	75,2	59,8	62,0
Fus-MAE w/ XAE&D	59,6	93,6	71,5	59,6	60,1

Table 2. Classification report for the SEN12MS dataset. S1 = SAR data only. S2 = optical data only. S1+S2 = SAR-optical data fusion. XAD = XAttnDecoder, XAE&D = XAttnEncoder&Decoder

4. EXPERIMENTS AND RESULTS

Benchmark setup - To study two different fusion strategies, we pretrained two instances of Fus-MAE: Fus-MAE w/ XAD, which only performs feature-level fusion, and Fus-MAE w/XAE&D, which performs both early and feature-level fusion. We train our models for 100 epochs on the 354,196 images the the BigEarthNet training split, applying the AdamW optimizer with batch size 200. The learning rate is warmed up to $1,5625 \times 10^{-4}$ for the 10 first epochs, and then decayed with a cosine schedule. We train our models on 2 NVIDIA RTX 3090Ti, for about 60 hours. We set ImageNet initialization as a baseline, and complete our benchmark with two pretrained Transformer-based models that were specifically designed for SAR-optical data fusion: DINO-MM [24] and SatViT [15], respectively representing recent studies in contrastive learning and masked image modelling.

Multilabel classification - To evaluate the effectiveness of our pretraining strategies, we append a linear classifier head on top of our pretrained encoder. We finetune the model over 10 epochs, using the MultiLabelSoftMargin Loss from PyTorch and the AdamW optimizer, and report the mean average precision (mAP) score over the test split. Table 1 summarizes the outcome of these finetuning experiments, where the classifier is trained on unimodal data (S1 or S2) or multimodal data (S1+S2). Notably, Fus-MAE demonstrates superior performance compared to the other architectures, achieving a substantial increase in mAP of approximately 2 percentage points for S2 and S1+S2, with the Fus-MAE w/XAE&D having a slight edge. It is however noteworthy that, across all architectures, the mAP using only SAR data (S1) is significantly lower than when using S2 or S1+S2, suggesting that all models mainly rely on optical data

for their predictions in the S1+S2 scenario. Additionally, to assess the quality of the learned representations under label-and resource-scarce conditions, we perform a linear evaluation on 1% of the training labels. In this scenario, the linear patch projection and the encoder weights are frozen, allowing only the weights of the linear classifier to be learned. We train this classifier for 20 epochs, with a batch size of 128, still utilizing the AdamW optimizer. Results are also reported on Table 1, revealing an even larger performance increase compared to other SSL architectures, highlighting the quality of the learned representations of our models.

Transfer learning - To study the generalization potential, we perform a linear evaluation on another downstream task: unimodal land-cover classification on the SEN12MS dataset [12]. Given the unbalanced nature of this dataset, we computed the precision, the recall and the F1-score using the weighted average method. We train this classifier for 10 epochs, with a batch size of 256, applying the LabelSmoothingCrossEntropy loss from Timm. Results of a benchmark with a similar setup as the previous experiment are reported on Table 2. Our models also outperform other techniques across all tracked metrics, although by a thinner margin.

5. CONCLUSION

In this paper, we introduce Fus-MAE, a novel SSL framework for SAR-optical data fusion. Based on a MAE architecture, it uses cross-attention between two data streams at different stages to perform early and feature-level data fusion. Our model outperforms recent contrastive learning and MIM-based works on various downstream tasks, demonstrating the effectiveness of using cross-attention to describe cross-modal

interactions between modalities with a large domain gap. Further research can be conducted to adapt our cross-attention layers to more than 2 modalities and to balance the prediction reliance of our model more evenly between the modalities.

6. REFERENCES

- [1] Shuran Song, Samuel P Lichtenberg, and Jianxiong Xiao, “Sun rgb-d: A rgb-d scene understanding benchmark suite,” in *Proceedings of the IEEE conference on computer vision and pattern recognition*, 2015, pp. 567–576.
- [2] Alec Radford, Jong Wook Kim, Chris Hallacy, Aditya Ramesh, Gabriel Goh, Sandhini Agarwal, Girish Sastry, Amanda Askell, Pamela Mishkin, Jack Clark, et al., “Learning transferable visual models from natural language supervision,” in *International conference on machine learning*. PMLR, 2021, pp. 8748–8763.
- [3] Yu Huang, Chenzhuang Du, Zihui Xue, Xuanyao Chen, Hang Zhao, and Longbo Huang, “What makes multi-modal learning better than single (provably),” *Advances in Neural Information Processing Systems*, vol. 34, pp. 10944–10956, 2021.
- [4] Patrick Ebel, Yajin Xu, Michael Schmitt, and Xiao Xiang Zhu, “Sen12ms-cr-ts: A remote-sensing data set for multimodal multitemporal cloud removal,” *IEEE Transactions on Geoscience and Remote Sensing*, vol. 60, pp. 1–14, 2022.
- [5] Sergio Vitale, Davide Cozzolino, Giuseppe Scarpa, Luisa Verdoliva, and Giovanni Poggi, “Guided patch-wise nonlocal sar despeckling,” *IEEE Transactions on Geoscience and Remote Sensing*, vol. 57, no. 9, pp. 6484–6498, 2019.
- [6] Alec Radford, Karthik Narasimhan, Tim Salimans, Ilya Sutskever, et al., “Improving language understanding by generative pre-training,” 2018.
- [7] Jacob Devlin, Ming-Wei Chang, Kenton Lee, and Kristina Toutanova, “Bert: Pre-training of deep bidirectional transformers for language understanding,” *arXiv preprint arXiv:1810.04805*, 2018.
- [8] Ting Chen, Simon Kornblith, Mohammad Norouzi, and Geoffrey Hinton, “A simple framework for contrastive learning of visual representations,” in *International conference on machine learning*. PMLR, 2020, pp. 1597–1607.
- [9] Kaiming He, Xinlei Chen, Saining Xie, Yanghao Li, Piotr Dollár, and Ross Girshick, “Masked autoencoders are scalable vision learners,” in *Proceedings of the IEEE/CVF conference on computer vision and pattern recognition*, 2022, pp. 16000–16009.
- [10] Oscar Manas, Alexandre Lacoste, Xavier Giró-i Nieto, David Vazquez, and Pau Rodriguez, “Seasonal contrast: Unsupervised pre-training from uncurated remote sensing data,” in *Proceedings of the IEEE/CVF International Conference on Computer Vision*, 2021, pp. 9414–9423.
- [11] Gencer Sumbul, Arne de Wall, Tristan Kreuziger, Filipe Marcelino, Hugo Costa, Pedro Benevides, Mário Caetano, Begüm Demir, and Volker Markl, “Bigearthnet-mm: A large-scale, multimodal, multilabel benchmark archive for remote sensing image classification and retrieval [software and data sets],” *IEEE Geoscience and Remote Sensing Magazine*, vol. 9, no. 3, pp. 174–180, 2021.
- [12] Michael Schmitt, Lloyd Haydn Hughes, Chunping Qiu, and Xiao Xiang Zhu, “Sen12ms—a curated dataset of georeferenced multi-spectral sentinel-1/2 imagery for deep learning and data fusion,” *arXiv preprint arXiv:1906.07789*, 2019.
- [13] Yi Wang, Nassim Ait Ali Braham, Zhitong Xiong, Chenying Liu, Conrad M Albrecht, and Xiao Xiang Zhu, “Ssl4eo-s12: A large-scale multi-modal, multi-temporal dataset for self-supervised learning in earth observation,” *arXiv preprint arXiv:2211.07044*, 2022.
- [14] Chao Tao, Ji Qi, Mingning Guo, Qing Zhu, and Haifeng Li, “Self-supervised remote sensing feature learning: Learning paradigms, challenges, and future works,” *IEEE Transactions on Geoscience and Remote Sensing*, vol. 61, pp. 1–26, 2023.
- [15] Anthony Fuller, Koreen Millard, and James R Green, “Satvit: Pretraining transformers for earth observation,” *IEEE Geoscience and Remote Sensing Letters*, vol. 19, pp. 1–5, 2022.
- [16] Limeng Zhang, Zenghui Zhang, Weiwei Guo, Tao Zhang, and Wenxian Yu, “3dmae: Joint sar and optical representation learning with vertical masking,” *IEEE Geoscience and Remote Sensing Letters*, 2023.
- [17] Ngoc Long Nguyen, Jérémie Anger, Axel Davy, Pablo Arias, and Gabriele Facciolo, “Self-supervised multi-image super-resolution for push-frame satellite images,” in *Proceedings of the IEEE/CVF Conference on Computer Vision and Pattern Recognition*, 2021, pp. 1121–1131.
- [18] Yezhen Cong, Samar Khanna, Chenlin Meng, Patrick Liu, Erik Rozi, Yutong He, Marshall Burke, David Lobell, and Stefano Ermon, “Satmae: Pre-training transformers for temporal and multi-spectral satellite imagery,” *Advances in Neural Information Processing Systems*, vol. 35, pp. 197–211, 2022.

[19] Carl Doersch, Abhinav Gupta, and Alexei A Efros, “Unsupervised visual representation learning by context prediction,” in *Proceedings of the IEEE international conference on computer vision*, 2015, pp. 1422–1430.

[20] Gustav Larsson, Michael Maire, and Gregory Shakhnarovich, “Colorization as a proxy task for visual understanding,” in *Proceedings of the IEEE conference on computer vision and pattern recognition*, 2017, pp. 6874–6883.

[21] Kaiming He, Haoqi Fan, Yuxin Wu, Saining Xie, and Ross Girshick, “Momentum contrast for unsupervised visual representation learning,” in *Proceedings of the IEEE/CVF conference on computer vision and pattern recognition*, 2020, pp. 9729–9738.

[22] Yuxing Chen and Lorenzo Bruzzone, “Self-supervised sar-optical data fusion of sentinel-1/-2 images,” *IEEE Transactions on Geoscience and Remote Sensing*, vol. 60, pp. 1–11, 2021.

[23] Antonio Montanaro, Diego Valsesia, Giulia Fracastoro, and Enrico Magli, “Semi-supervised learning for joint sar and multispectral land cover classification,” *IEEE Geoscience and Remote Sensing Letters*, vol. 19, pp. 1–5, 2022.

[24] Yi Wang, Conrad M Albrecht, and Xiao Xiang Zhu, “Self-supervised vision transformers for joint sar-optical representation learning,” in *IGARSS 2022-2022 IEEE International Geoscience and Remote Sensing Symposium*. IEEE, 2022, pp. 139–142.

[25] Mathilde Caron, Hugo Touvron, Ishan Misra, Hervé Jégou, Julien Mairal, Piotr Bojanowski, and Armand Joulin, “Emerging properties in self-supervised vision transformers,” in *Proceedings of the IEEE/CVF international conference on computer vision*, 2021, pp. 9650–9660.

[26] Xian Sun, Peijin Wang, Wanxuan Lu, Zicong Zhu, Xiaonan Lu, Qibin He, Junxi Li, Xuee Rong, Zhujun Yang, Hao Chang, et al., “Ringmo: A remote sensing foundation model with masked image modeling,” *IEEE Transactions on Geoscience and Remote Sensing*, 2022.

[27] Matt Allen, Francisco Dorr, Joseph A Gallego-Mejia, Laura Martínez-Ferrer, Anna Jungbluth, Freddie Kalaitzis, and Raúl Ramos-Pollán, “Large scale masked autoencoding for reducing label requirements on sar data,” *arXiv preprint arXiv:2310.00826*, 2023.

[28] Roman Bachmann, David Mizrahi, Andrei Atanov, and Amir Zamir, “Multimae: Multi-modal multi-task masked autoencoders,” in *European Conference on Computer Vision*. Springer, 2022, pp. 348–367.

[29] Alexey Dosovitskiy, Lucas Beyer, Alexander Kolesnikov, Dirk Weissenborn, Xiaohua Zhai, Thomas Unterthiner, Mostafa Dehghani, Matthias Minderer, Georg Heigold, Sylvain Gelly, et al., “An image is worth 16x16 words: Transformers for image recognition at scale,” *arXiv preprint arXiv:2010.11929*, 2020.